State-Space Averaged Modeling of a Nonideal Boost Converter.

C.A. Nwosu, M.Eng.

Department of Electrical Engineering, University of Nigeria, Nsukka, Nigeria.

E-mail: cajethannwosu@yahoo.com

ABSTRACT

Design-oriented analysis of switching converters must take into account how disturbances and variations in the input and control signals affect the optimum performance of these converters. Sate-space averaging of a nonideal boost converter is presented in this paper. DC state and small signal AC state modeling of the converter was derived. Determination of line-to-output transfer function, which describes how variations or disturbances in the applied voltage lead to disturbances in the output voltage, control-to-output transfer function, which describes how control input variations influence the output voltage, and input and output impedances of the converters, which play a significant role when an electromagnetic interference (EMI) filter is added at the converter power input are the areas of application of small-signal equivalent circuit model of a switching converter derived from the state space modeling of converters.

(Keywords: switching converters, performance, boost converters, line-to-output, control-to-output, EMI)

INTRODUCTION

Modeling of a system may be described as a process of formulating a mathematical description of the system [1]. It entails the establishment of a mathematical input-output model which best approximates the physical reality of a system [2]. In control systems (which are dynamic physical systems) this entails obtaining the differential equations of the systems by the appropriate applications of relevant laws of nature. Switching converters are nonlinear systems (i.e., systems which may be modeled by sequential but not simultaneous equations). Even when the system is modeled by a set of simultaneous equations, one of the equations must at least be nonlinear. The equations are nonlinear because they usually involve the manipulation of nonlinear quantities [3].

The nonlinearity of switching converters makes it desirable that small-signal linearized models be constructed. An advantage of such linearized model is that for constant duty cycle, it is time invariant: there is no switching or switching ripple to deal with, and only the important DC components of the waveforms are modeled. This is achieved by perturbing and linearizing the average model about a quiescent operating point [3].

The sate-space averaging method, different from the circuit averaging technique (circuit averaging approach involves manipulation of circuits rather than equations), is a mainstay of modern control theory. The state-space averaging method makes use of the state-space description of dynamical systems to derive the small-signal averaged equations of PWM switching converters. A benefit of the state-space averaging procedure is the generality of its result: a small-signal averaged model can always be obtained, provided that state equations of the original converter can be written [3].

LINEARIZATION OF THE STATIC CONTROL-TO-INPUT CHARACTERISTIC OF THE BOOST CONVERTER

Full-wave diode rectifier network, cascaded by a continuous conduction mode (CCM) DC-DC boost converter has been developed [3] – [8], for the realization of a near-ideal rectifier system. These rectifiers involve the variation of the converter duty cycle, as necessary to cause the converter input current $i_{ac}(t)$ to be proportional to the applied input voltage $v_{ac}(t)$ as shown in Equation (1):

$$i_{ac} = \frac{v_{ac}(t)}{R_e} \quad \textbf{(1)}$$

where R_e is constant of proportionality, also known as the emulated resistance. For a sinusoidal applied input voltage $v_{ac}(t)$ given by:

$$v_{ac}(t) = V_m \sin(\omega t) \quad \textbf{(2)}$$

The rectified voltage $v_r(t)$ is:

$$v_r(t) = V_m |\sin(\omega t)| \quad \textbf{(3)}$$

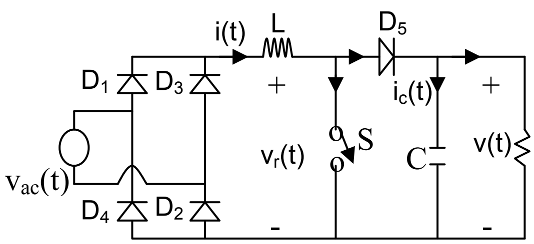

Figure 1: Full-Wave Rectifier Cascaded by a Boost Converter.

Normally, it is desired that the converter output voltage be a constant DC value v(t) = V. The converter conversion ratio must therefore be:

$$M(d(t)) = \frac{v(t)}{v_r(t)} = \frac{V}{V_m|\sin(\omega t)|} \quad \textbf{(4)}$$

If the boost converter operates in continuous conduction mode, and if the inductor is small enough that its influence on the low frequency components of the converter waveforms is negligible, then the duty ratio should follow the relation:

$$M(d(t)) = \frac{1}{1-d(t)} \quad \textbf{(5)}$$

Equations (4) and (5), imply that the duty ratio should follow the function:

$$d(t) = 1 - \frac{v_r(t)}{V} \quad \textbf{(6)}$$

Figure 2 shows the nonlinear characteristics of a boost converter, obtained from Equation (6), for $v_r(t) \le V$. The Figure illustrates the variation of the duty cycle with the instantaneous value of the rectified voltage for a given regulated output voltage. At a quiescent duty cycle, say 0.5, we construct a linear function about the quiescent operating pint. The linearized model satisfies the relation:

$$\frac{1}{1-D} = \frac{V}{V_r} \quad \textbf{(7)}$$

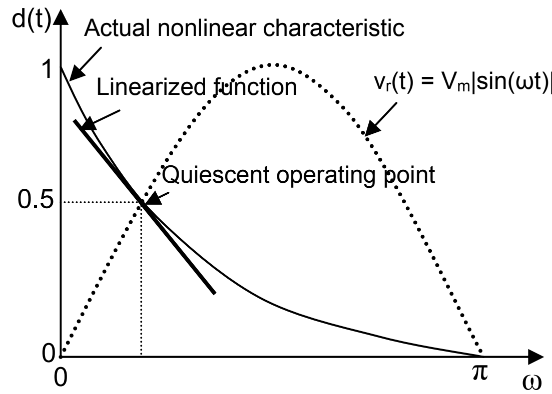

Figure 2: Boost Converter Nonlinear Characteristic.

For a quiescent input voltage Vr, variation in duty cycle $\hat{d}$ about the quiescent operating duty cycle D, will excite variations $\hat{v}$ in the output voltage. If the magnitude of the duty cycle variation is sufficiently small, then we can compute the resulting output voltage variation linearizing the curve. Thus the linearized and nonlinear functions, will exhibit an approximately same characteristics provided that the duty cycle variations $\hat{d}$ are sufficiently small.

STATE SPACE AVERAGING OF A NONIDEAL BOOST CONVERTER

Consider the boost converter of Figure 3. The physical state variables are the independent inductor current i(t) and the capacitor voltage v(t), thus we define the state vector x(t) as:

$$x(t) = \begin{vmatrix} i(t) \\ v(t) \end{vmatrix} \quad \textbf{(8)}$$

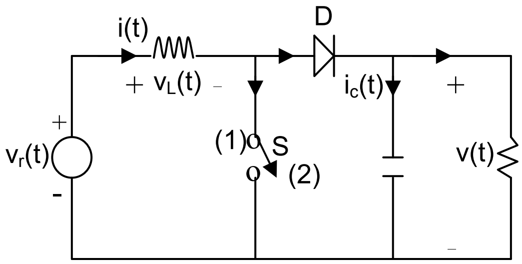

Figure 3: Boost Converter Circuit.

In modeling the nonideal boost converter, the conduction loss of MOSFET, Q (represented by switch S in Figure 3), is modeled by on resistance R_{on}, while the forward voltage drop of diode D is modeled by an independent voltage source of value V_D.

The input voltage $v_r(t)$ is an independent source which should be placed in the input vector u(t). In addition, the modeled diode forward voltage drop V_D is also included in the input vector u(t). Thus, we define the input vector as:

$$u(t) = \begin{vmatrix} v_r(t) \\ V_D \end{vmatrix} \qquad \textbf{(9)}$$

To model the converter input port, we need to find the converter input current $i_r(t)$. To calculate this dependent current, it should be included in the output vector y(t). Thus, we define the output vector as:

$$y(t) = |i_r(t)| \qquad \textbf{(10)}$$

Here it isn't necessary to include the output voltage v(t) in the output vector y(t), since v(t) is already included in the state vector x(t).

Our interest is to represent the converter system in state equations of the form:

$$K\frac{dx(t)}{dt} = Ax(t) + Bu(t)$$
$$y(t) = Cx(t) + Eu(t) \qquad \textbf{(11)}$$

where K is a matrix containing the values of capacitance, inductance, and mutual inductance (if any), such that Kdx(t)/dt is a vector containing the inductor winding voltages and capacitor currents. The matrices A, B, C, and E contain constants of proportionality.

We now write the state equations for each interval of the switching of the converter. When the switch is in position (1), the converter circuit of Figure 4(a) is obtained.

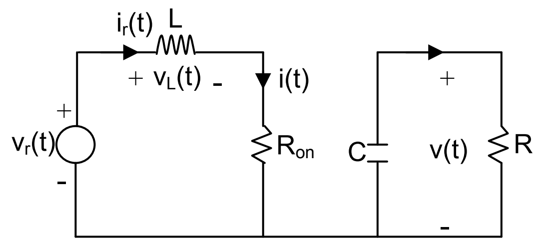

(a)

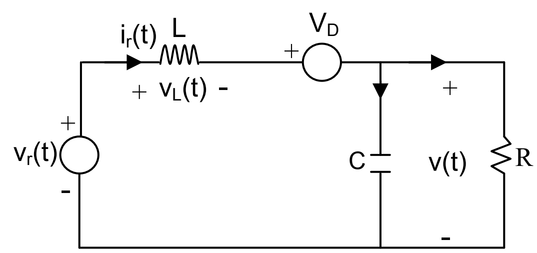

(b)

Figure 4: Boost Converter Circuit (a) During Subinterval 1 (b) During Subinterval 2.

The inductor voltage, capacitor current and converter input current are:

$$L\frac{di(t)}{dt} = v_r(t) - i(t)R_{on}$$
$$C\frac{dv(t)}{dt} = \frac{-v(t)}{R} \qquad \textbf{(12)}$$
$$i_r(t) = i(t)$$

These equations can be written in the following state-space form:

$$\underbrace{\begin{bmatrix} L & 0 \\ 0 & C \end{bmatrix}}_{K}\underbrace{\frac{d}{dt}\begin{bmatrix} i(t) \\ v(t) \end{bmatrix}}_{\frac{dx(t)}{dt}} = \underbrace{\begin{bmatrix} -R_{on} & 0 \\ 0 & -\frac{1}{R} \end{bmatrix}}_{A_1}\underbrace{\begin{bmatrix} i(t) \\ v(t) \end{bmatrix}}_{x(t)} + \underbrace{\begin{bmatrix} 1 & 0 \\ 0 & 0 \end{bmatrix}}_{B_1}\underbrace{\begin{bmatrix} v_r(t) \\ V_D \end{bmatrix}}_{u(t)}$$

$$\underbrace{[i_r(t)]}_{y(t)} = \underbrace{[1 \quad 0]}_{C_1}\underbrace{\begin{bmatrix} i(t) \\ v(t) \end{bmatrix}}_{x(t)} + \underbrace{[0 \quad 0]}_{E_1}\underbrace{\begin{bmatrix} v_r(t) \\ V_D \end{bmatrix}}_{u(t)} \qquad \textbf{(13)}$$

When the switch is in position (2), the converter circuit of Figure 4(b) is obtained.

The inductor voltage, capacitor current and converter input current are:

$$L\frac{di(t)}{dt} = v_r(t) - v(t) - V_D$$
$$C\frac{dv(t)}{dt} = i(t) - \frac{v(t)}{R} \qquad \textbf{(14)}$$
$$i_r(t) = i(t)$$

The state-space equation representations of these equations are:

$$\underbrace{\begin{bmatrix} L & 0 \\ 0 & C \end{bmatrix}}_{K}\underbrace{\frac{d}{dt}\begin{bmatrix} i(t) \\ v(t) \end{bmatrix}}_{\frac{dx(t)}{dt}} = \underbrace{\begin{bmatrix} 0 & -1 \\ 1 & -\frac{1}{R} \end{bmatrix}}_{A_2}\underbrace{\begin{bmatrix} i(t) \\ v(t) \end{bmatrix}}_{x(t)} + \underbrace{\begin{bmatrix} 1 & -1 \\ 0 & 0 \end{bmatrix}}_{B_2}\underbrace{\begin{bmatrix} v_r(t) \\ V_D \end{bmatrix}}_{u(t)}$$

$$\underbrace{[i_r(t)]}_{y(t)} = \underbrace{[1 \quad 0]}_{C_2}\underbrace{\begin{bmatrix} i(t) \\ v(t) \end{bmatrix}}_{x(t)} + \underbrace{[0 \quad 0]}_{E_2}\underbrace{\begin{bmatrix} v_r(t) \\ V_D \end{bmatrix}}_{u(t)}$$

(15)

DC STATE MODELING

Here provisions are made that the natural frequencies of the converter, as well as the frequencies of variations of the converter inputs, are much slower than the switching frequency. By this end, the state-space averaged model that describes the converter in equilibrium is:

$$0 = AX + BU$$
$$Y = CX + EU \qquad \textbf{(16)}$$

where X = equilibrium (DC) state vector
U = equilibrium (DC) input vector
Y = equilibrium (DC) output vector

The averaged matrices are given by:

$$A = DA_1 + D'A_2$$
$$B = DB_1 + D'B_2$$
$$C = DC_1 + D'C_2 \qquad \textbf{(17)}$$
$$E = DE_1 + D'E_2$$

where D = equilibrium (DC) duty cycle.

We now evaluate the state-space averaged equilibrium equations. The averaged matrix A is:

$$A = DA_1 + D'A_2$$
$$= D\begin{bmatrix} -R_{on} & 0 \\ 0 & -1/R \end{bmatrix} + D'\begin{bmatrix} 0 & -1 \\ 1 & -1/R \end{bmatrix} = \begin{bmatrix} -DR_{on} & -D' \\ D' & -1/R \end{bmatrix}$$

(18)

In a similar manner, the averaged matrices B, C, and E are evaluated as follows:

$$B = DB_1 + D'B_2$$
$$= D\begin{bmatrix} 1 & 0 \\ 0 & 0 \end{bmatrix} + D'\begin{bmatrix} 1 & -1 \\ 0 & 0 \end{bmatrix} = \begin{bmatrix} 1 & -D' \\ 0 & 0 \end{bmatrix} \qquad \textbf{(19)}$$

$$C = DC_1 + D'C_2 = D[1 \quad 0] + D'[1 \quad 0] = [1 \quad 0] \qquad \textbf{(20)}$$

$$E = DE_1 + D'E_2 = D[0 \quad 0] + D'[0 \quad 0] = [0 \quad 0] \qquad \textbf{(21)}$$

The DC state Equation (19) therefore become:

$$\begin{bmatrix} 0 \\ 0 \end{bmatrix} = \begin{bmatrix} -DR_{on} & -D' \\ D' & -1/R \end{bmatrix}\begin{bmatrix} I \\ V \end{bmatrix} + \begin{bmatrix} 1 & -D' \\ 0 & 0 \end{bmatrix}\begin{bmatrix} V_r \\ V_D \end{bmatrix}$$
$$[I_r] = [1 \quad 0]\begin{bmatrix} I \\ V \end{bmatrix} + [0 \quad 0]\begin{bmatrix} V_r \\ V_D \end{bmatrix} \qquad \textbf{(22)}$$

Equation (16) can be solved to find the equilibrium state and output vectors as follows:

$$X = -A^{-1}BU$$
$$Y = (-CA^{-1}B + E)U \qquad \textbf{(23)}$$

and when applied to Equation (22), the equilibrium state and output vectors are:

$$\begin{bmatrix} I \\ V \end{bmatrix} = \left(\frac{1}{1 + \frac{DR_{on}}{D'^2 R}}\right)\begin{bmatrix} \frac{1}{D'^2 R} & -\frac{1}{D'R} \\ -\frac{1}{D'} & 1 \end{bmatrix}\begin{bmatrix} V_s \\ V_D \end{bmatrix}$$

$$[I_s] = \left(\frac{1}{1 + \frac{DR_{on}}{D'^2 R}}\right)\begin{bmatrix} \frac{1}{D'^2 R} & -\frac{1}{D'R} \end{bmatrix}\begin{bmatrix} V_s \\ V_D \end{bmatrix}$$

(24)

Expansion of top row of Equation (22) yields:

$$V_r - D'V_D - DR_{on}I - D'V = 0 \qquad \textbf{(25)}$$

while expansion of the second row of Equation (22) yields:

$$D'I - V/R = 0 \qquad \textbf{(26)}$$

Equivalent circuits corresponding to Equations (25) and (26) are shown in Figures 5 and 6, respectively.

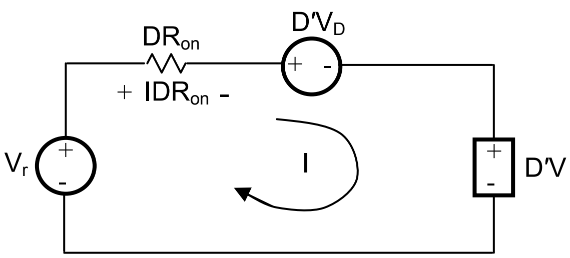

Figure 5: Equivalent Circuit Corresponding to Equation 25.

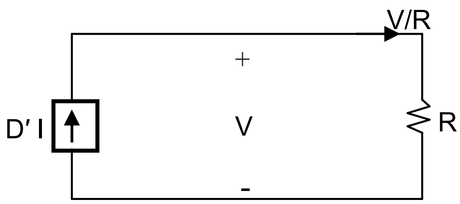

Figure 6: Equivalent Circuit Corresponding to Equation 26.

The two circuits of Figure 5 and Figure 6 are drawn together in Figure 7. The dependent sources $D'V$ and $D'I$ are combined into an ideal D':1 transformer in Figure 8, yielding the complete DC equivalent circuit model.

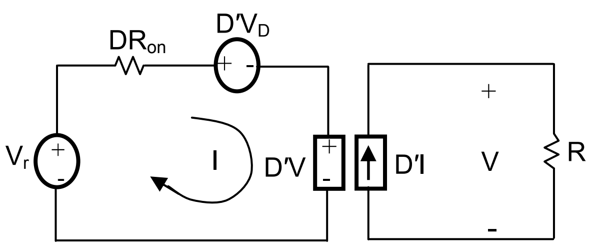

Figure 7: The Circuits of Figure 5 and Figure 6 Drawn Together.

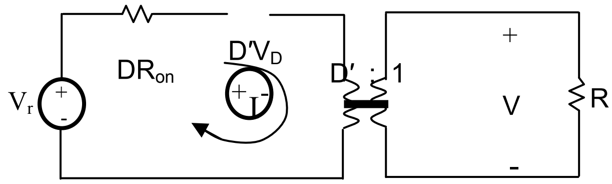

Figure 8: Equivalent DC Circuit Model of the Boost Converter of Figure 2, Including Ideal DC Transformer and MOSFET and Diode Conduction Losses.

SMALL-SIGNAL AC STATE MODELING

The switching ripple is usually small in a well-designed converter operating in continuous conduction mode (CCM). Hence we neglect the switching ripple, and model only the underlying AC variations in the converter waveforms. The switching ripples in the inductor current and capacitor voltage waveforms are removed by averaging over one switching period. Hence, the low-frequency components of the inductor and capacitor waveforms are modeled by equations of the form:

$$L\frac{d\langle i_L(t)\rangle_{Ts}}{dt} = \langle v_L(t)\rangle_{Ts}$$
$$C\frac{d\langle v_c(t)\rangle_{Ts}}{dt} = \langle i_c(t)\rangle_{Ts} \qquad \textbf{(27)}$$

where $\langle x(t)\rangle_{Ts}$ denotes the average of x(t) over an interval of length Ts:

$$\langle x(t)\rangle_{Ts} = \frac{1}{Ts}\int_t^{t+Ts} x(\tau)d\tau \qquad \textbf{(28)}$$

Thus, the average value is allowed to vary from one switching period to the next, such that low-frequency variations are modeled. In effect, the "moving average" of Equation (28) constitutes low pass filtering of the waveform as illustrated in Figure 9 [3]. Still, the averaged inductor voltage and capacitor current of Equation (27) are, in general, nonlinear functions of the signals in the converter, and are therefore, a set of nonlinear differential equations.

To obtain a linear model that is easier to analyze, we construct a small signal that has been linearized about a quiescent operating point such that the characteristics of the linearized and nonlinear functions are approximately equal for sufficiently small variations in $\hat{v}(t)$ say, about V.

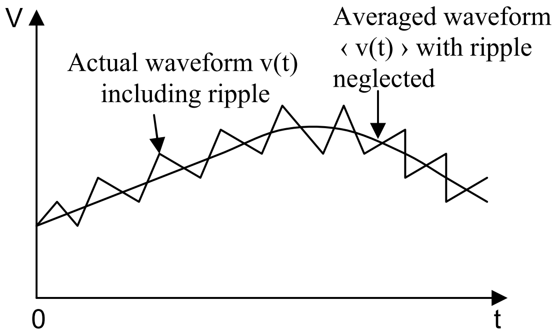

Figure 9: Converter Output Voltage Waveform.
(Here, the actual waveform v(t), including high-frequency switching ripple, and its averaged, low-frequency component, <v(t)>$_{Ts}$ are illustrated).

Thus, the equations of the small-signal AC model are:

$$K\frac{d\hat{x}(t)}{dt} = A\hat{x}(t) + B\hat{u}(t) + \{(A_1 - A_2)X + (B_1 - B_2)U\}\hat{d}(t)$$
$$\hat{y}(t) = C\hat{x}(t) + E\hat{u}(t) + \{(C_1 - C_2)X + (E_1 - E_2)U\}\hat{d}(t) \quad \textbf{(29)}$$

where the quantities $\hat{x}(t), \hat{u}(t), \text{and } \hat{d}(t)$ in Equation (29) are small AC variations about the equilibrium solution, or quiescent operating point defined by Equations (16) to (23).

The small-signal model of our example boost converter is found by evaluation of Equation (29). First, the vector coefficients of $\hat{d}(t)$ are:

$$(A_1 - A_2)X + (B_1 - B_2)U = \begin{bmatrix} V - IR_{on} \\ -I \end{bmatrix} + \begin{bmatrix} V_D \\ 0 \end{bmatrix} = \begin{bmatrix} V - IR_{on} + V_D \\ -I \end{bmatrix} \quad \textbf{(30)}$$
$$(C_1 - C_2)X + (E_1 - E_2)U = [0]$$

The small-signal AC state equations (29) therefore become:

$$\begin{bmatrix} L & 0 \\ 0 & C \end{bmatrix}\frac{d}{dt}\begin{bmatrix} \hat{i}(t) \\ \hat{v}(t) \end{bmatrix} = \begin{bmatrix} -DR_{on} & -D' \\ D & -1/R \end{bmatrix}\begin{bmatrix} \hat{i}(t) \\ \hat{v}(t) \end{bmatrix} + \begin{bmatrix} 1 & -D' \\ 0 & 0 \end{bmatrix}\begin{bmatrix} \hat{v}(t) \\ 0 \end{bmatrix} + [V - IR_{on} + V_D]\hat{d}(t) \quad \textbf{(31)}$$
$$[\hat{i}_r(t)] = [1 \quad 0]\begin{bmatrix} \hat{i}(t) \\ \hat{v}(t) \end{bmatrix} + [0 \quad 0]\begin{bmatrix} \hat{v}_r(t) \\ 0 \end{bmatrix}$$

The diode forward voltage drop is modeled as a constant value V_D. To this end, there are no AC variations in this source, and $\hat{v}_D(t)$ equals zero. When written in scalar form, Equation (31) becomes:

$$L\frac{d\hat{i}(t)}{dt} = -D'\hat{v}(t) - DR_{on}\hat{i}(t) + \hat{v}_r(t) + (V - IR_{on} + V_D)\hat{d}(t) \quad \textbf{(32)}$$
$$C\frac{d\hat{v}(t)}{dt} = D'\hat{i}(t) - \frac{\hat{v}(t)}{R} - I\hat{d}(t)$$
$$\hat{i}_r(t) = \hat{i}(t)$$

Circuits corresponding to Equation (32) are listed in Figure 10, while these circuits are combined into the complete small-signal AC equivalent circuit model of Figure 11.

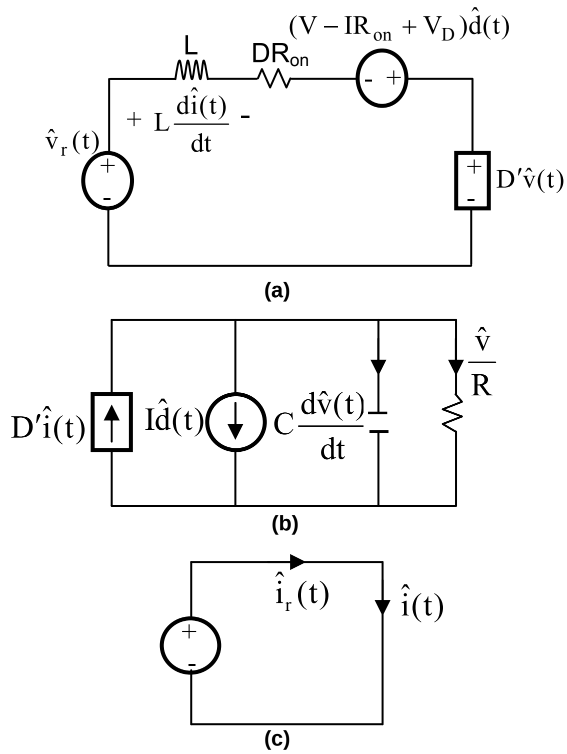

Figure 10: Circuits Equivalent to the Small-Signal Converter Equations (a) Inductor Loop, (b) Capacitor Node, and (c) Input Port.

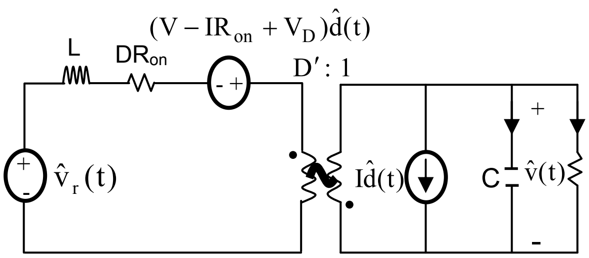

Figure 11: Complete Small-Signal Equivalent Circuit Model of a Nonideal Boost Converter Example.

CONCLUSIONS

State-space averaging of a nonideal boost converter has been presented in this paper. DC equivalent and small-signal equivalent circuit models of nonideal boost converter were derived. The resulting small-signal equivalent circuit model can be analyzed using standard conventional linear circuit techniques, such as the Laplace transform, to gain insight into the behavior and properties of the converter which include for example, the origins of the frequency response of complex converter systems. Other benefits of small-signal equivalent circuit model of a switching converter are that it makes simpler, by the application of relevant circuit analyses method, the determination of:

(1) The line-to-output transfer function, which describes how variations or disturbances in the applied voltage lead to disturbances in the output voltage.

(2) The control-to-output transfer function, which describes how control input variations influence the output voltage.

(3) The input impedance, which plays a significant role when an electromagnetic interference (EMI) filter is added at the converter power input. The output impedance, which describes how variations in the load current affect the output voltage, etc.

REFERENCES

1. Thaler, G.J. 1989. *Automatic Control System*. West Publishing Company: St. Paul, MN.

2. Fargeon, C. 1989. *The Digital Control of Systems*. Van Nostrand Reinhold: New York, NY.

3. Erickson, R.W. and D. Maksinovic. 2001. *Fundamentals of Power Electronics*. Kluwer Academic Publishers: Norwell, MA.

4. Van der Berg, M. and J.A. Ferreira. 1998. “A Family of Low EMI Unity Power Factor Converters”. *IEEE Trans. Power Electronics*. 13(3):547-555.

5. Kim, S. and P.N. Enjeti. 2004. “A Parallel-Connected Single Phase Power Factor Correction Approach With Improve Efficiency”. *IEEE Trans. Power Electronics*. 19(1):87-93.

6. Zane, R. and D. Maksimovic. 1998. “Nonlinear–Carrier Control for High Power: Factor Rectifiers Based on Up–Down Switching Converters”. *IEEE Trans. Power Electronics*. 13(2):213 – 221.

7. Yip, S.C., D.Y. Qui, H. Shu-Hung Chung. and S.Y.R. Hui. 2003. “A Novel Voltage Sensorless Control Technique for a Bidirectional AC/DC Converter”. *IEEE Trans. Power Electronics*. 18:1346-1355.

8. Garcia, O., J.A. Cobos, R. Prieto, P. Alou, and J. Uceda. 2003. “Single Phase Power Factor Correction: A Survey”. *IEEE Trans. Power Electronics*. 18(3):749-755.

ABOUT THE AUTHOR

Cajethan A. Nwosu obtained his B.Eng. and M.Eng. degrees in Electrical Engineering from University of Nigeria, Nsukka, Nigeria, in 1994 and 2004, respectively. He is presently working toward his Ph.D. degree in Electrical Engineering. He is currently a lecturer in the Department of Electrical Engineering, University of Nigeria, Nsukka, Nigeria. His research interests include power electronic converters and renewable energy technologies.

SUGGESTED CITATION

Nwosu, C.A. 2008. “State-Space Averaged Modeling of a Nonideal Boost Converter”. *Pacific Journal of Science and Technology*. 9(2):302-308.

Pacific Journal of Science and Technology